

Parameters Variability Effects on Microstrip Interconnects via Hermite Polynomial Chaos

*Original*

Parameters Variability Effects on Microstrip Interconnects via Hermite Polynomial Chaos / Manfredi, Paolo; Stievano, IGOR SIMONE; Canavero, Flavio. - STAMPA. - (2010), pp. 149-152. (Intervento presentato al convegno 19th IEEE Conference on Electrical Performance of Electronic Packaging and Systems, EPEPS tenutosi a Austin, TX (USA) nel Oct. 25-27, 2010) [10.1109/EPEPS.2010.5642568].

*Availability:*

This version is available at: 11583/2373680 since:

*Publisher:*

IEEE

*Published*

DOI:10.1109/EPEPS.2010.5642568

*Terms of use:*

openAccess

This article is made available under terms and conditions as specified in the corresponding bibliographic description in the repository

*Publisher copyright*

(Article begins on next page)

# Parameters Variability Effects on Microstrip Interconnects via Hermite Polynomial Chaos

Paolo Manfredi, Igor S. Stievano, Flavio G. Canavero

Dipartimento di Elettronica, Politecnico di Torino  
10129 Torino, Italy (igor.stievano@polito.it)

**Abstract**—This paper focuses on the derivation of an enhanced transmission-line model allowing to describe a realistic high-speed interconnect with the inclusion of external uncertainties, like tolerances or process variations. The proposed method, that is based on the expansion of the well-known telegraph equations in terms of Hermite polynomials, turns out to be accurate and more efficient than alternative solutions like Monte Carlo in determining the transmission-line response sensitivity to parameters variability. Two application examples involving the frequency-domain analysis of realistic PCB microstrip structures conclude the paper.

**Index Terms**—Circuit modeling, Circuit Simulation, Transmission-lines, Stochastic analysis, tolerance analysis, Uncertainty.

## I. INTRODUCTION

Nowadays, simulation techniques allowing for the analysis of high-speed digital links with the inclusion of the effects of possible uncertainties of the circuit parameters are highly desirable, in view of the urging necessity to perform right-the-first-time designs. The stochastic analysis of a digital link is a tool that is extremely useful in the early design phase for the prediction of the system performance and for setting realistic design margins.

The typical resource allowing to collect quantitative information on the statistical behavior of the circuit response is based on the application of the brute-force Monte Carlo (MC) method, or possible complementary methods based on the optimal selection of the subset of model parameters in the whole design space [1]. Such methods, however, are computationally expensive, and this fact prevents us from their application to the analysis of complex realistic structures.

Recently, an effective solution that overcomes the previous limitation, has been proposed. This methodology is based on the polynomial chaos (PC) theory [2], [3] and on the representation of the stochastic solution of a dynamical circuit in terms of orthogonal polynomials. This technique enjoys applications in several domains of Physics; we limit ourselves to mention recent results on the extension of the classical circuit analysis tools, like the modified nodal analysis (MNA), to the prediction of the stochastic behavior of circuits with uncertain parameters [4], [5], [6]. However, so far, the application has been limited to dynamical circuits consisting only of lumped elements.

In this paper, the original contribution consists in the application of PC theory to new devices, whose behavior

is regulated by a different class of differential equations; in particular we will show the case of long and distributed interconnects described by transmission-line equations [7]. This will allow the stochastic analysis of realistic structures combining lumped circuits and distributed interconnects, as required by the simulation of high-speed digital links. The feasibility and strength of the approach is demonstrated on a realistic printed circuit board (PCB) structure.

## II. HERMITE POLYNOMIAL CHAOS

This Section provides the essential mathematical background of the proposed method.

The idea underlying the polynomial chaos technique resides in the representation of a stochastic process via the sum of orthogonal basis functions. Within this framework, a *generic* stochastic process  $H$ , that in our specific application will be the frequency-domain response of a transmission-line, can be approximated by means of the following truncated series

$$H(\xi) = \sum_{k=0}^P H_k \cdot \phi_k(\xi) \quad (1)$$

where  $\{\phi_k\}$  are Hermite polynomials expressed in terms of the standard Gaussian variable  $\xi$  with zero mean and unit variance and  $\{H_k\}$  are the linear coefficients of the expansion. As an example, the first three polynomials are  $\phi_0 = 1$ ,  $\phi_1 = \xi$ ,  $\phi_2 = (\xi^2 - 1)$ .

For a given process, approximation (1) is defined by the number of terms  $P$  (limited to the range  $2 \div 5$  for practical applications) and by the expansion coefficients that are computed via the projection of  $H$  onto the orthogonal components  $\phi_0$ ,  $\phi_1$ ,  $\dots$ . The orthogonality property of Hermite polynomials is expressed by

$$\langle \phi_k, \phi_j \rangle = \langle \phi_k^2 \rangle \delta_{kj} \quad (2)$$

where  $\delta_{kj}$  is the Kronecker delta and  $\langle \cdot, \cdot \rangle$  denotes the inner product in the Hilbert space of the variable  $\xi$  with Gaussian weighting function, *i.e.*,

$$\langle \phi_k, \phi_j \rangle = \int_{-\infty}^{+\infty} \phi_k(\xi) \phi_j(\xi) \exp(-\xi^2/2) / (\sqrt{2\pi}) d\xi. \quad (3)$$

A comprehensive and formal discussion of polynomial chaos, including the generalization of (1) to multiple random variables, is available in [2], [3] and references therein.

### III. STOCHASTIC TRANSMISSION-LINE EQUATIONS

This section discusses the modification of the classical transmission line equations, as needed for incorporating the effects of the statistical variation of the per-unit-length (p.u.l.) parameters via the polynomial chaos theory.

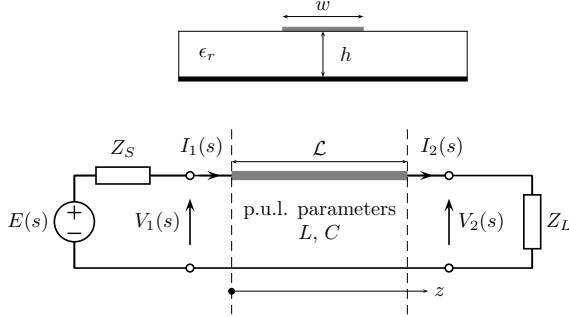


Fig. 1. Microstrip test structure considered to demonstrate the proposed approach. Top panel: crosssection; bottom panel: simulation test case.

For the sake of simplicity, the discussion is based on a lossless two-conductor line as the microstrip structure shown in Fig. 1 that is governed by the following equation in the Laplace domain [7] .

$$\frac{d}{dz} \begin{bmatrix} V(z, s) \\ I(z, s) \end{bmatrix} = -s \begin{bmatrix} 0 & L \\ C & 0 \end{bmatrix} \begin{bmatrix} V(z, s) \\ I(z, s) \end{bmatrix} \quad (4)$$

In the above equation,  $s$  is the Laplace variable,  $V$  and  $I$  are the transverse voltage and current variables in the longitudinal  $z$  direction and  $C$  and  $L$  are the p.u.l. capacitance and inductance, depending on the geometrical and material properties of the structure.

The expansion (1) of the p.u.l parameters and of the unknown voltage and current variables in terms of Hermite polynomials, yields a modified version of (4), that for the second row of the equation becomes

$$\begin{aligned} \frac{d}{dz} (I_0(z, s)\phi_0 + I_1(z, s)\phi_1 + I_2(z, s)\phi_2) = \\ -s(C_0\phi_0 + C_1\phi_1 + C_2\phi_2)(V_0(z, s)\phi_0 + \\ + V_1(z, s)\phi_1 + V_2(z, s)\phi_2) \end{aligned} \quad (5)$$

where a second-order expansion (*i.e.*,  $P = 2$ ) is assumed; the indexed electrical variables and p.u.l.'s in the above equation represent the expansion coefficients.

Projection of (5) and of the companion relation arising from the first row of (4) on the first three Hermite polynomials leads to the following augmented system, where the random variable  $\xi$  does not explicitly appear,

$$\frac{d}{dz} \begin{bmatrix} \mathbf{V}(z, s) \\ \mathbf{I}(z, s) \end{bmatrix} = -s \begin{bmatrix} 0 & \mathbf{L} \\ \mathbf{C} & 0 \end{bmatrix} \begin{bmatrix} \mathbf{V}(z, s) \\ \mathbf{I}(z, s) \end{bmatrix} \quad (6)$$

In the above equation, vectors  $\mathbf{V} = [V_0, V_1, V_2]^T$  and  $\mathbf{I} = [I_0, I_1, I_2]^T$  collect the different coefficients of the polynomial

chaos expansion of the voltage and current variables. The new p.u.l. matrix  $\mathbf{C}$  turns out to be

$$\mathbf{C} = \begin{bmatrix} C_0 & C_1 & 2C_2 \\ C_1 & C_0 + 2C_2 & 2C_1 \\ C_2 & C_1 & C_0 + 4C_2 \end{bmatrix}. \quad (7)$$

and a similar relation holds for matrix  $\mathbf{L}$ .

It is worth noting that equation (6) belongs to the same class of (4) and plays the role of the set of equations of a multiconductor transmission-line with a number of conductors that is  $(P + 1)$  times larger than those of the original line. However, for small values of  $P$  (as typically occurs in practice), the additional overhead in handling the augmented equations is much less than the time required to run a large number of MC simulations. Extension of (4) to the general case of a multiconductor lossy line is straightforward.

### IV. BOUNDARY CONDITIONS AND SIMULATION

For the deterministic case, the simulation of an interconnect like the one of Fig. 1 amounts to combining the port electrical relations of the two terminal elements defining the source and load with the transmission-line equation, and solving the system. This is a standard procedure as illustrated for example in [7] (see Ch.s 4 and 5).

Similarly, when the problem becomes stochastic, the augmented transmission-line equation (6) is used in place of (4) together with the projection of the characteristics of the source and the load elements on the first  $P + 1$  Hermite polynomials. For the example of Fig. 1, the augmented port equations of the line terminations become

$$\begin{cases} \mathbf{V}_1(s) = [E(s), 0, 0]^T - Z_S(s)\mathbf{I}_2(s) \\ \mathbf{V}_2(s) = Z_L(s)\mathbf{I}_2(s) \end{cases} \quad (8)$$

where the port voltages and currents need to match the solutions of the differential equation (6) at line ends (*e.g.*,  $\mathbf{V}_1(s) = \mathbf{V}(z=0, s)$ ,  $\mathbf{V}_2(s) = \mathbf{V}(z=L, s)$ ).

Once the unknown voltages and currents are computed, the quantitative information on the spreading of circuit responses can be readily obtained from the analytical expression of the unknowns. As an example, the frequency-domain solution of the magnitude of voltage  $V_1$ , arising from (8) and (6) with  $P = 2$ , leads to  $|V_1(j\omega)| = |V_{10}(j\omega) + V_{11}(j\omega)\xi + V_{12}(j\omega)(\xi^2 - 1)|$ . The above relation, that turns out to be a known nonlinear function of the random variable  $\xi$ , can be used to compute the PDF of  $|V_1(j\omega)|$  via numerical simulation or analytical formulae.

### V. NUMERICAL RESULTS

In this Section, the proposed technique is applied to the analysis of two realistic interconnect structures.

*Example 1.* The first example is the microstrip of Fig. 1, where  $w = 100\mu\text{m}$ ,  $h = 60\mu\text{m}$ ,  $t = 35\mu\text{m}$ ,  $L = 5\text{ cm}$ . The source and load elements are defined according to the notation in (8) with  $Z_S = R_S = 50\Omega$  and  $Z_L = 1/(sC_L + G_L)$ , being  $C_L = 10\text{ pF}$ ,  $G_L = 1/(10\text{ k}\Omega)$ .

In this example, the variability is provided by the relative permittivity  $\epsilon_r$ , that is assumed to behave as a Gaussian random variable with 3.7 mean value and 10% relative standard deviation. The approximate relations given in [7] have been used to compute the third-order PC expansion of the unknowns and of the p.u.l. parameters of the structure ( $L_0 = 3.3$  nH/cm,  $L_1 = L_2 = L_3 = 0$ ,  $C_0 = 1.72$  pF/cm,  $C_1 = 0.125$  pF/cm and  $C_2 = C_3 = 0$ ).

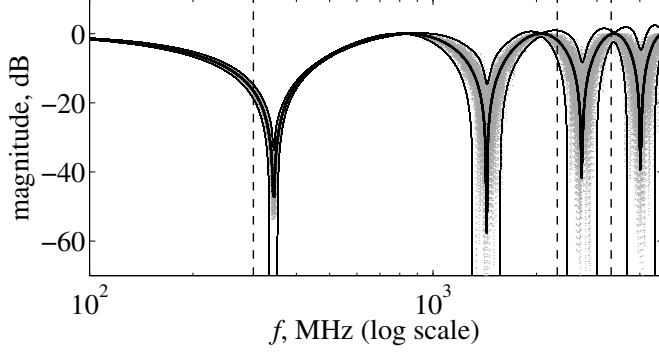


Fig. 2. Bode plots (magnitude) of the transfer function  $H(j\omega) = V_1(j\omega)/E(j\omega)$  of the first example test case (see text for details). Solid black thick line: deterministic response; solid black thin lines:  $3\sigma$  tolerance limit of the third order polynomial chaos expansion; gray lines: a sample of responses obtained by means of the MC method (limited to 100 curves, for graph readability).

Figure 2 shows a comparison of the Bode plot (magnitude) of the transfer function  $H(j\omega) = V_1(j\omega)/E(j\omega)$  computed via the advocated PC method and determined by means of MC procedure. The solid black thin curves of Fig. 2 represent the  $\pm 3\sigma$  interval of the transfer function, determined from the results of the proposed technique. For comparison, the deterministic response with nominal values of the circuit elements is reported in Fig. 2 as a solid black thick line; also, a limited set of MC simulations (100, out of the 40,000 runs, in order not to clutter the figure) are plotted as gray lines. Clearly, the thin curves of Fig. 2 provide a qualitative information of the spread of responses due to parameters uncertainty.

A better quantitative prediction is also possible from the knowledge of the actual PDF of the network response. This fact can be clearly appreciated in Fig. 3, by comparing the PDF of  $|H(j\omega)|$  computed for different frequencies over 40,000 MC simulations, and the distribution obtained from the analytical PC expansion of  $V_1(j\omega)/E(j\omega)$ . The frequencies selected for this comparison correspond to the dashed lines shown in Fig. 2. The good agreement between the actual and the predicted PDFs and, in particular, the accuracy in reproducing the tails and the large variability of non-gaussian shapes of the reference distributions, confirm the potential of the proposed method. In addition, for this example, it is also clear that a PC expansion with three terms is already accurate enough to capture the dominant statistical information of the system response.

**Example 2.** The second example is a coupled microstrip structure, where the length, width, thickness and terminations

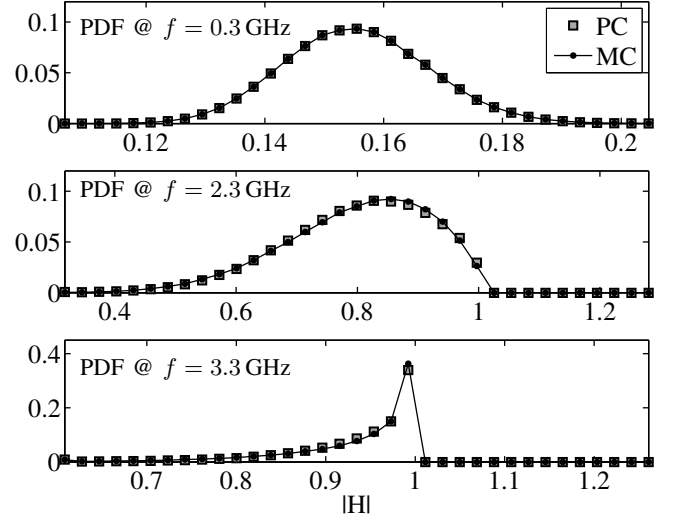


Fig. 3. Probability density function of  $|H(j\omega)|$  of Example 1, computed at different frequencies. Of the two distributions, the one marked MC refers to 40000 MC simulations, and the one marked PC refers to the response obtained via third order polynomial chaos expansion.

of the traces are the same used in the previous scalar example. Also, one line is active and the other is quiet and kept in the low state, *i.e.*, the corresponding voltage source at the near-end is zero. The variability is provided by the relative permittivity  $\epsilon_r$  and the trace separation  $s$ , that are assumed to behave as two independent Gaussian random variables  $\xi_1$  and  $\xi_2$  with 3.7 and  $80\mu\text{m}$  mean values, respectively, and identical 10% relative standard deviation. The approximate relations collected in [8] have been used to compute the third-order PC expansion of the unknowns and of the p.u.l. parameters of the structure. For the sake of brevity, the formal development of PC theory for multiple variables, inspired by [2], [3], is omitted here.

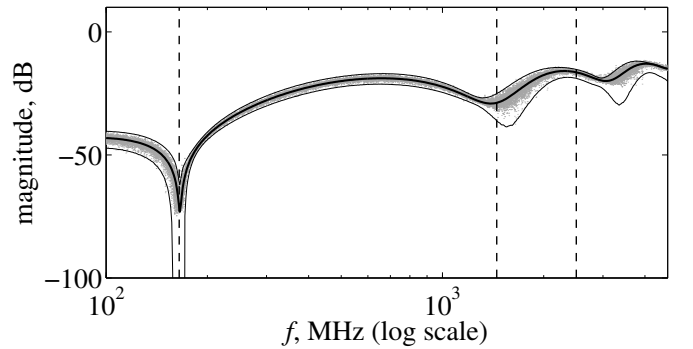


Fig. 4. Bode plots (magnitude) of the near-end crosstalk transfer function  $H(j\omega)$  of the second example test case (see text for details). Solid black thick line: deterministic response; solid black thin lines:  $3\sigma$  tolerance limit of the third order polynomial chaos expansion; gray lines: a sample of responses obtained by means of the MC method (limited to 100 curves, for graph readability).

As already done in the scalar example, Figure 4 shows

a comparison of the Bode plot (magnitude) of the transfer function  $H(j\omega)$  defining the near-end crosstalk computed via the advocated PC method and determined by means of the MC procedure. The same notation used in Figure 2 is adopted. The thin curves of Fig. 4 provide a qualitative information of the spread of responses due to parameters uncertainty. A better quantitative prediction can be appreciated in Fig. 5, that compares the PDF of  $|H(j\omega)|$  computed for different frequencies over 40,000 MC simulations, and the distribution obtained via the analytical PC expansion. The frequencies selected for this comparison correspond to the dashed lines shown in Fig. 4. The good agreement between the actual and the predicted PDFs for this alternative example confirm the strengths of the proposed method.

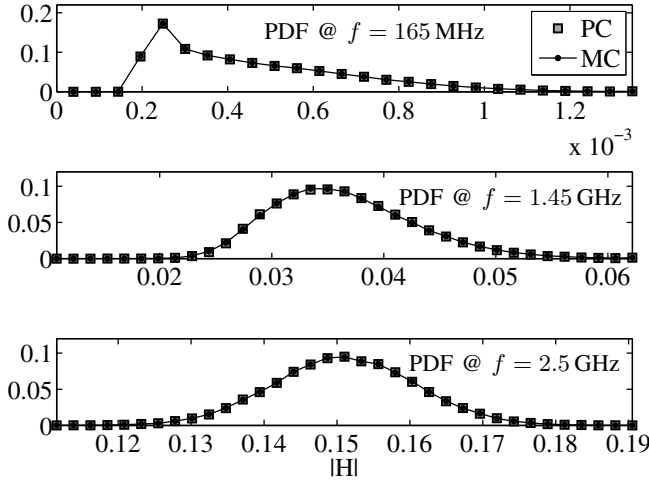


Fig. 5. Probability density function of  $|H(j\omega)|$  for Example 2, computed at different frequencies. Of the two distributions, the one marked MC refers to 40000 MC simulations, and the one marked PC refers to the response obtained via third order polynomial chaos expansion.

In addition, Fig. 6 shows the surface of  $|H(j\omega)|$  computed at  $f = 2.5$  GHz as a function of the two random variables  $\xi_1$  and  $\xi_2$ , corresponding to relative permittivity and trace separation, respectively. The comparison between the actual surface and the one predicted via the PC method for a predefined order  $P$  of the expansion is provided as well. The two plots in the figure correspond to a third and a fifth order of the PC expansion, thus highlighting that the expansion order  $P$  can be effectively used to improve the accuracy of the approximation for a wide range of parameter variability.

## VI. CONCLUSIONS

The generation of an enhanced transmission-line equation describing a realistic interconnect structure with the inclusion of external uncertainties is addressed in this paper. The proposed method is based on the expansion of the voltage and current variables into a sum of a limited number of orthogonal basis functions, leading to an extended set of telegraph equations. The advocated method, while providing accurate

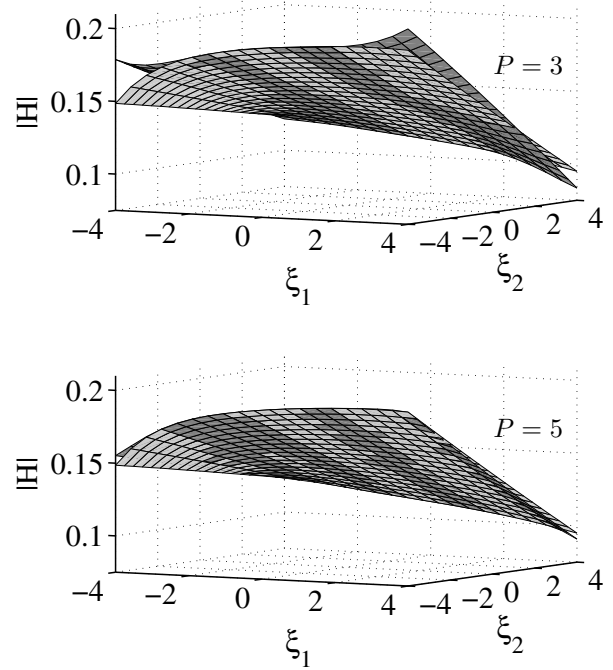


Fig. 6. Plot of  $|H(j\omega)|$  at  $f = 2.5$  GHz as a function of the two random parameters, *i.e.*, the relative permittivity and the trace separation. Light gray: reference; dark gray: PC approximation. The two panels represent the results obtained with different expansion orders (3 and 5).

results, turns out to be more efficient than the classical Monte Carlo technique in determining the transmission-line response sensitivity to parameters variability. The strenght of the proposed technique is demonstrated by means of two realistic PCB microstrip structures and frequency-domain analysis.

## REFERENCES

- [1] Q. Zhang, J. J. Liou, J. McMacken, J. Thomson, P. Layman, "Development of robust interconnect model based on design of experiments and multiobjective optimization," *IEEE Transactions on Electron Devices*, Vol. 48, No. 9, pp. 1885 – 1891, Sep. 2001.
- [2] D. Xiu, G. E. Karniadakis, "The Wiener-Askey polynomial chaos for stochastic differential equations," *SIAM, Journal of Sci. Computation*, Vol. 24, No. 2, pp. 619–622, 2002.
- [3] B. J. Deusschere et Al., "Numerical challenges in the use of polynomial chaos representations for stochastic processes," *SIAM Journal on Scientific Computing*, Vol. 26, No. 2, pp. 698–719, 2005
- [4] K. Strunz, Q. Su, "Stochastic formulation of SPICE-type electronic circuit simulation using polynomial chaos," *ACM Transactions on Modeling and Computer Simulation*, Vol. 18, No. 4, Sep. 2008.
- [5] Y. Zou et Al., "Practical implementation of stochastic parametrized model order reduction via Hermite polynomial chaos," *Proc. of the 2007 Asia and South Pacific Design Automation Conference*, pp. 367–372, 2007.
- [6] I. S. Stievano, F. G. Canavero, "Response Variability of High-Speed Interconnects via Hermite Polynomial Chaos," *Proc. of the 14th IEEE Workshop on Signal Propagation on Interconnects*, Hildesheim, Germany, pp. 3-6, May 09-12, 2010.
- [7] C. R. Paul, "Analysis of Multiconductor Transmission Lines," Wiley, 1994.
- [8] B. C. Wadell "Transmission Line Design Handbook," Artech House, 1991.